Bridging of liquid drops at chemically structured walls

Alexandr Malijevský

Department of Physical Chemistry, University of Chemical Technology Prague, Praha 6, 166 28, Czech Republic
and Department of Molecular and Mesoscopic Modelling, ICPF of the Czech Academy Sciences, Prague 165 02, Czech Republic

Andrew O. Parry

Department of Mathematics, Imperial College London, London SW7 2BZ, United Kingdom

Martin Pospíšil

Department of Physical Chemistry, University of Chemical Technology Prague, Praha 6, 166 28, Czech Republic
and Department of Molecular and Mesoscopic Modelling, ICPF of the Czech Academy Sciences, Prague 165 02, Czech Republic

Using mesoscopic interfacial models and microscopic density functional theory we study fluid adsorption at a dry wall decorated with three completely wet stripes of width L separated by distances D_1 and D_2. The stripes interact with the fluid with long-range forces inducing a large finite-size contribution to the surface free energy. We show that this nonextensive free-energy contribution scales with $\ln L$ and drives different types of bridging transition corresponding to the merging of liquid drops adsorbed at neighboring wetting stripes when the separation between them is *molecularly* small. We determine the surface phase diagram and show that this exhibits two triple points, where isolated drops, double drops, and triple drops coexist. For the symmetric case, $D_1 = D_2 \equiv D$, our results also confirm that the equilibrium droplet configuration always has the symmetry of the substrate corresponding to either three isolated drops when D is large or a single triple drop when D is small; however, symmetry-broken configurations do occur in a metastable part of the phase diagram which lies very close to the equilibrium-bridging phase boundary. Implications for phase transitions on other types of patterned surface are considered.

I. INTRODUCTION

The study of fluid adsorption and droplet formation on structured and patterned surfaces has received a great deal of attention in recent years. This is in part motivated by practical applications such as microfluidics [1] and superhydrophobicity [2,3] and also, more fundamentally, by the many new types of interfacial phase transitions [4–19] that can occur compared to those at structureless and chemically homogeneous surfaces [20–23]. Consider, for example, a flat substrate (wall) decorated with one or more stripes which have an enhanced wettability, that is, a lower contact angle θ, compared to the rest of the wall, which serves to preferentially nucleate liquid. When the volume of liquid is fixed, such surfaces can induce macroscopic morphological phase transitions associated with the local breaking of translational invariance and Young's law [24,25]. In the grand canonical ensemble, that is, when the volume of liquid is not constrained, morphological transitions do not occur since the fluid density profile must have the same symmetry as the confining external field induced by the wall. However, in their place are a number of phase transitions including the possibility of the formation of liquid bridges that span between different striped regions when the gaps between them are sufficiently small [26]. These are similar to bridging transitions, that is, the local condensation of liquid, between nanoparticles (spheres, cylinders, etc.) immersed in a solvent reservoir [27–31].

In the present paper we study bridging transitions on a chemically heterogeneous surface decorated with three identical stripes of width L that are completely wet (contact angle $\theta = 0$). This topography allows, in principle, for stable and metastable droplet and bridging configurations which either follow or break the symmetry of the substrate. Our motivation is not only to show that bridging transitions must occur as the distance between the stripes is reduced but also that these occur in such a way as to suppress the possibility of equilibrium spontaneous symmetry breaking associated with different bridgelike coverings of the wall which occur only in a metastable part of the phase diagram. However, as we will see, the quantitative nature of the metastability is quite surprising with repercussions for the structure of the phase diagram. Our paper is arranged as follows: in Sec. II we use simple scaling and interfacial Hamiltonian theory to predict equilibrium droplet configurations on a dry surface decorated with one, two, and three stripes which are completely wet. We focus on systems with long-ranged dispersion-like forces for which there are important finite-size contributions to the surface free energy of drop configurations. For a surface with three stripes we distinguish between symmetric and broken symmetric droplet shapes and determine the location of different possible phase transitions between them. In this way, we are able to predict the phase diagram when we vary the distances D_1 and D_2 between the stripes. In Sec. III we confirm these predictions using microscopic density functional

theory where we specialize to a perfectly dry wall patterned with wet stripes. We finish with a discussion concerning generalizations and repercussions for phase transitions on periodically decorated substrates.

II. INTERFACE HAMILTONIAN MODEL

To begin, we recall briefly the features of a drop nucleated at a single stripe and in particular why, for systems with dispersion-like forces, there is a logarithmic contribution to the excess surface free energy. This is crucial when considering the quantitative aspects of the different bridging phase boundaries when the substrate is decorated with more stripes. Consider a planar wall in contact with vapor at chemical potential μ close to saturation μ_{sat} at temperature T far below the bulk critical value T_c. The wall is partially wet by liquid, corresponding to contact angle θ, except along a macroscopically long, deep stripe of width L, which is made of a different material that is completely wet. The stripe nucleates a liquid drop which remains of finite height h_m, even at saturation chemical potential, which depends on the stripe width. Simple finite-size scaling arguments predict that at saturation $h_m \propto L^{\beta_s^{co}/\nu_\parallel^{co}}$ where β_s^{co} and $\nu_\parallel^{co}$ are, respectively, the critical exponents for the adsorption and parallel correlation length characterizing a complete wetting phase transition [20–22,26,32]. Similarly the surface free energy per unit length of the stripe should contain a singular contribution $f_s \propto L^{1-(2-\alpha_s^{co})/\nu_\parallel^{co}}$ where now α_s^{co} is the surface specific heat exponent. For systems with long-ranged dispersion forces the upper critical dimension for complete wetting $d_{co}^* < 3$, so that in three dimensions the mean-field values of the critical exponents $\alpha_s^{co} = 4/3$, $\beta_s^{co} = 1/3$, and $\nu_\parallel^{co} = 2/3$ are exact [33]. This predicts that the droplet height scales as $h_m \propto \sqrt{L}$, while the exponent for the free energy *vanishes*, suggesting that this is a marginal case allowing for logarithmic corrections. These scaling predictions contrast with the situation for systems with short-ranged forces for which we anticipate $h_m \propto \ln L$ and $f_s \propto 1/L^2$.

These scaling considerations are completely in accord with calculations based on a mesoscopic interfacial Hamiltonian model

$$H[h] = \int dx \left\{ \frac{\gamma}{2} \left(\frac{dh}{dx} \right)^2 + W(h) \right\}, \tag{1}$$

where $h(x)$ is the height of the drop above the stripe which extends from $x = -L/2$ to $x = L/2$, γ is the liquid-gas surface tension, and $W(h)$ is the binding potential. Translational invariance is assumed for the drop height along the stripe, and the binding potential at bulk coexistence is assumed to take the same form, $W(h) = A/h^2$, as for a uniform completely wet substrate where A is the (positive) Hamaker constant. This assumption is justified since the drop height is much smaller than the length L. Since the region outside the stripe is partially wet we may impose that the drop height is fixed to a small, microscopic value at the edges $x = \pm L/2$. In three dimensions interfacial fluctuation effects at complete wetting are near negligible and a mean-field treatment of interfacial model suffices to determine the drop shape. Minimization

of (1) leads to the Euler-Lagrange equation [21]

$$\gamma \frac{d^2 h}{dx^2} = W'(h), \tag{2}$$

which is easily solved for the drop shape. For wide stripes this leads to the scaling solution

$$h(x) = h_m \sqrt{1 - 4x^2/L^2}, \tag{3}$$

where the midpoint height is determined as [26]

$$h_m^2 \approx L \sqrt{\frac{A}{2\gamma}}, \tag{4}$$

in accord with the scaling prediction above. These mean-field results are not altered by the inclusion of interfacial fluctuations associated with the thermal wandering of the interface. For example we can anticipate these induce a near negligible interfacial roughness at the midpoint, which scales as $\sqrt{\ln L}$, which is much smaller than the equilibrium height h_m. Evaluating $H[h]$ for the equilibrium profile shape determines that the surface free energy per unit length of this single drop behaves as

$$F_{drop}(L) = \gamma L + \sqrt{2A\gamma} \ln L + \cdots, \tag{5}$$

which indeed shows the logarithmic correction to the surface free energy. The fact that this contribution diverges with L means it is not possible to define edge or line tension contributions to the surface free energy of the drop. This is very different from the case with purely short-ranged forces for which the analogous finite-size correction is of order $1/L$. Returning to the case of long-ranged forces, taking a derivative w.r.t. L determines that the force of solvation induced by the drop on the edges of the stripe is $f_{sol} = \gamma + O(1/L)$. The finite-size correction to the surface tension here can be interpreted as a critical Casimir force induced by the complete wetting of the stripe, which is characterized by a large correlation length associated with interfacial fluctuations which is limited only by the value of the width L.

Next consider two completely wet stripes, each of width L, separated by a distance D. In this case two interfacial configurations are possible [see Fig. 1(b)]. If the distance D is large, the stripes are independent and isolated drops form on them. The excess surface free energy associated with this configuration is well approximated by $2F_{drop}(L) + \gamma_{wg}D$. The last contribution here arises from the surface tension associated with the wall-gas configuration above the region between the stripes. However, if the distance D is sufficiently small, we may imagine that a single drop bridges between the stripes with associated surface free energy $F_{drop}(2L) + (\gamma_{wl} + \gamma)D$. This approximation is justified if $D \ll L$, which is indeed the case near the bridging transition. Matching these free energies determines that these configurations coexist when the width between the stripes is equal to

$$D_B = \frac{1}{1 - \cos\theta} \sqrt{\frac{2A}{\gamma}} \ln L + \cdots, \tag{6}$$

where we recall that θ is the contact angle above the nonwet parts away from the striped regions and the higher order
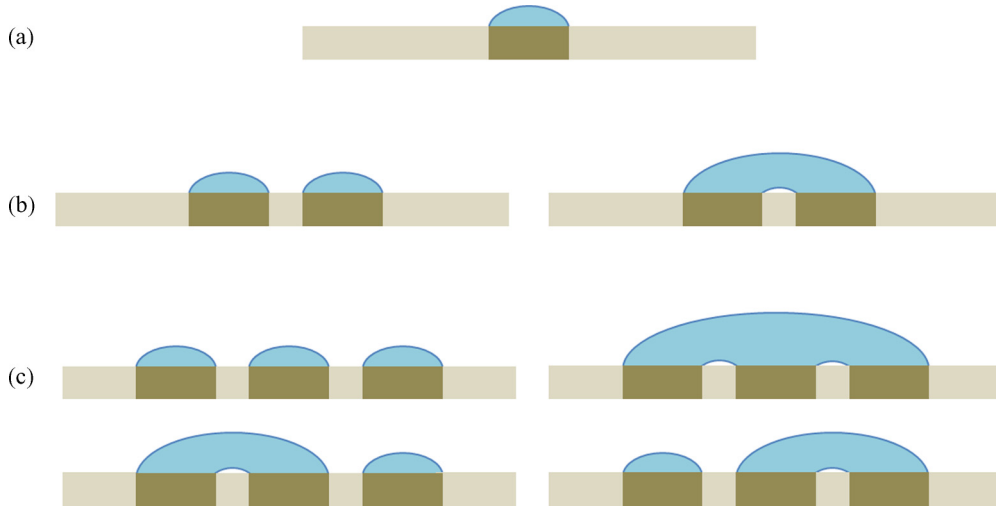
FIG. 1. Schematic illustration of possible isolated or bridging droplet configurations on a dry substrate ($\theta = \pi$) decorated with (a) one, (b) two, or (c) three completely wet stripes of width L.

terms remain finite as L increases. Beyond the present mean-field analysis we anticipate that sharp, first-order bridging transitions are rounded due to fluctuation effects. However, the scale of the rounding is small, of order $\exp(-\gamma D h_m / k_B T)$, which, even for microscopic systems, is negligible away from the bulk critical temperature [34].

Finally we turn our attention to the case of three identical stripes separated by regions of width D_1 and D_2. To begin, we consider the symmetric situation $D_1 = D_2 = D$, which will be sufficient to determine the structure of the phase diagram. Depending on the width D there are conceivably four possible droplet configurations [Fig. 1(c)]. If D is large, isolated drops cover the three wet stripes. From the considerations above it follows that for $D < D_B$ two of the drops coalesce to form a bridge over one of the dry regions. Clearly there are two equivalent ways of doing this which break the left or right symmetry of the substrate decoration (and underlying potential). However, this transition may or may not be preceded by the coalescence of all three drops into a single drop which bridges both dry regions, occurring at a distance D_B^*.

To determine D_B^* we again simply compare the surface free energy of a single bridging configuration with the value $3F_{\mathrm{drop}}(L) + 2\gamma_{wg}D$ corresponding to three isolated drops. Since we can anticipate that the value of $D_B^* \ll L$, we can approximate the free energy of the single bridging drop as $F_{\mathrm{drop}}(3L) + (2\gamma_{wl} + 2\gamma)D$. This implies that the value of D_B^* at which there is coexistence of the three isolated drops and the single triple drop is given by

$$D_B^* = D_B + \frac{1}{1 - \cos\theta}\sqrt{\frac{2A}{\gamma} \ln \frac{2}{\sqrt{3}}}. \quad (7)$$

This result can also be obtained by solving the Euler-Lagrange equation for the full interfacial model and matching solutions at the boundaries between the striped regions.

At this juncture we make a number of points.

First, as expected, the values D_B and D_B^* diverge as the contact angle θ vanishes, so that the entire wall is completely wet. Their values are smallest for $\theta = \pi$, that is, a dry wall, where

there is the maximum penalty to the free energy of bridging between the stripes. Although they diverge with L, the scale of D_B and D_B^* are set by the magnitude of the prefactor $\sqrt{A/\gamma}$, which, away from the near vicinity of the bulk critical temperature, is molecularly small. Thus, in general, bridging occurs only when the stripes are microscopically close to each other.

Second, as $D_B^* > D_B$ the coalescence of the three isolated drops into a single drop as D is reduced must precede the possible symmetry-breaking transition, which, if present, must occur in a metastable region of the phase diagram. This is in keeping with the general expectation that the equilibrium density profile of an inhomogeneous fluid must have the same symmetry as the confining external potential. It is intriguing, however, that the difference $D_B^* - D_B$ is small and independent of L, implying that the symmetry-breaking transition is only metastable. As L increases the locations of the equilibrium (three drops to one) and metastable but symmetry-breaking (three drops to a double drop) transition get relatively closer to each other. In the next section we shall show that even for microscopic systems the metastable transition still lies very close to the true equilibrium transition.

Finally, having determined that $D_B^* > D_B$ it follows that when the distances D_1 and D_2 between the stripes are unequal the phase diagram should have five first-order phase boundary lines and two triple points occurring for $D_1 \neq D_2$, which lie close to each other. At each triple point configurations corresponding to three isolated drops, a double bridging drop with an isolated drop and a single triple bridging drop all coexist. The fact that $D_B^* > D_B$ rules out the alternative possibility the triple points occur along the diagonal $D_1 = D_2$. The phase diagram will be determined explicitly in the next section using a more microscopic model DFT.

III. MICROSCOPIC DENSITY FUNCTIONAL THEORY

A. Microscopic model

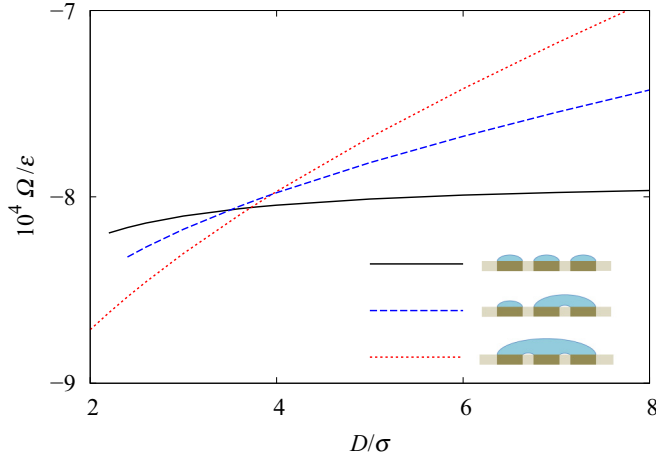Within DFT [35], the equilibrium state of an inhomogeneous fluid within the grand-canonical ensemble is

FIG. 2. DFT results showing the dependence of the grand potential on the stripe separation D for the symmetric situation when $D = D_1 = D_2$. In keeping with the predictions of the interfacial model as the distance D is reduced a single bridging transition occurs from three isolated drops to a single triple droplet. Also shown is the grand potential of a metastable symmetry-broken configuration with one double droplet which lies close to the global minimum in the vicinity of the equilibrium-bridging transition.

characterized by a one-body density profile $\rho(\mathbf{r})$. In general, the equilibrium distribution is obtained by minimizing the grand potential functional

$$\Omega[\rho] = \mathcal{F}[\rho] + \int d\mathbf{r} \rho(\mathbf{r})[V(\mathbf{r}) - \mu], \quad (8)$$

where $V(\mathbf{r})$ is the external potential. Here the intrinsic free energy functional $\mathcal{F}[\rho]$ can be separated into an exact ideal gas contribution and an excess part:

$$\mathcal{F}[\rho] = \beta^{-1} \int d\mathbf{r} \rho(\mathbf{r})\{\ln[\rho(\mathbf{r})\Lambda^3] - 1\} + \mathcal{F}_{ex}[\rho], \quad (9)$$

where Λ is the thermal de Broglie wavelength and $\beta = 1/k_B T$. As is common in modern DFT approaches, the excess part is modeled as a sum of hard-sphere and attractive contributions where the latter is treated in a standard mean-field fashion [36]:

$$\mathcal{F}_{ex}[\rho] = \mathcal{F}_{hs}[\rho] + \frac{1}{2} \iint d\mathbf{r}\, d\mathbf{r}' \rho(\mathbf{r})\rho(\mathbf{r}')u_a(|\mathbf{r} - \mathbf{r}'|), \quad (10)$$

where $u_a(r)$ is the attractive part of the fluid-fluid interaction potential.

In our model the fluid atoms are assumed to interact with one another via the truncated (i.e., short-ranged) and nonshifted Lennard-Jones-like potential

$$u_a(r) = \begin{cases} 0; & r < \sigma \\ -4\varepsilon\left(\frac{\sigma}{r}\right)^6; & \sigma < r < r_c, \\ 0; & r > r_c \end{cases} \quad (11)$$

which is cut off at $r_c = 2.5\,\sigma$, where σ is the hard-sphere diameter.

The hard-sphere part of the excess free energy is approximated using the (original) fundamental measure functional (FMT) [37],

$$\mathcal{F}_{hs}[\rho] = \frac{1}{\beta} \int d\mathbf{r}\, \Phi(\{n_\alpha\}), \quad (12)$$

which accurately takes into account the short-range correlations between the fluid particles. Here $\{n_\alpha\}$ are six weighted densities corresponding to fundamental measures of a sphere [37]. Although other prescriptions of Φ within modified versions of FMT are available [38], the original Rosenfeld FMT functional is perfectly adequate to describe the packing effects in the system under study.

The external field $V(\mathbf{r})$ is exerted by a planar wall occupying the volume $z < 0$. We specialize to the case $\theta = \pi$ for which we recall that the predicted values of D_B and D_B^* are smallest. This is very easily achieved by assuming that the wall is purely repulsive, except for three deep parallel stripes, each of width L. The total potential of the wall can thus be written as

$$V(x, z) = \begin{cases} \infty; & z < 0 \\ V_L(x, z) + V_L(x - D_1, z) \\ +V_L(x - D_1 - L - D_2, z); & z > 0, \end{cases} \quad (13)$$

where $V_L(x, z)$ is the potential due to a single stripe located at $0 < x < L$ and D_1 and D_2 are the distances between the stripes. Here we also assume that the stripes are macroscopically long, so that the system possesses translation invariance along the y axis.

We suppose that the stripes atoms are distributed uniformly within their domains with a particle density ρ_w and interact with the fluid particles via the Lennard-Jones 12-6 potential

$$\phi(r) = 4\varepsilon_w\left[\left(\frac{\sigma}{r}\right)^{12} - \left(\frac{\sigma}{r}\right)^6\right]. \quad (14)$$

The net potential $V_L(x, z)$ is obtained by summing up the wall-fluid pair potential over the wall volume of the stripe. Therefore

$$V_L(x, z) = \rho_w \int_{x-L}^{L} dx' \int_{-\infty}^{\infty} dy' \int_{z}^{\infty} dz'$$
$$\times \phi(\sqrt{x'^2 + y'^2 + z'^2}), \quad (15)$$

which can be expressed in the following scaling form:

$$V_L(x, z) = \pi \varepsilon_w \rho_w \sigma^3 \left[\frac{\sigma^9}{z^9}G_9\left(\frac{x}{z}, \frac{L}{z}\right) - \frac{\sigma^3}{z^3}G_3\left(\frac{x}{z}, \frac{L}{z}\right)\right] \quad (16)$$

with

$$G_9(\xi, \eta) = F_9(\xi - \eta) - F_9(\xi) \quad (17)$$

and

$$G_3(\xi, \eta) = F_3(\xi - \eta) - F_3(\xi), \quad (18)$$

where

$$F_9(\xi) = \frac{2}{45}\left(1 + \frac{1}{\xi^9}\right) - \frac{1}{2880}\frac{128\,\xi^{16} + 448\,\xi^{14} + 560\,\xi^{12} + 280\,\xi^{10} + 35\,\xi^8 + 280\,\xi^6 + 560\,\xi^4 + \xi^2 + 128}{\xi^9(1 + \xi^2)^{7/2}} \quad (19)$$
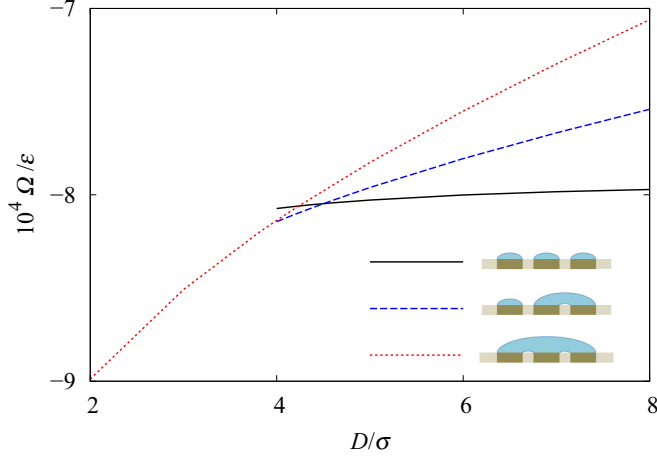
FIG. 3. Dependence of the grand potential on the separation $D = D_1 = D_2 - \sigma$ when the widths between the stripes are slightly different. In this case two bridging transitions, first from three isolated drops to a double bridging drop and then to a triple bridging droplet, occur as D is reduced.

and

$$F_3(\xi) = \frac{1}{3}\left[1 + \frac{1}{\xi^3} - \frac{2\xi^4 + \xi^2 + 2}{2\xi^3\sqrt{1+\xi^2}}\right]. \qquad (20)$$

Minimization of (8) leads to the Euler-Lagrange equation

$$V(\mathbf{r}) + \frac{\delta \mathcal{F}_{\mathrm{hs}}[\rho]}{\delta \rho(\mathbf{r})} + \int d\mathbf{r}' \rho(\mathbf{r}') u_{\mathrm{a}}(|\mathbf{r} - \mathbf{r}'|) = \mu, \qquad (21)$$

which we solve iteratively on a two-dimensional grid $(0, X) \times (0, Z)$ where we set $X = 200\,\sigma$ and $Z = 30\,\sigma$. The first stripe is situated within the interval $(x_i, x_i + L)$ where x_i satisfies $2x_i + 3L + D_1 + D_2 = X$. We impose the boundary conditions $\rho(x, z_m) = \rho_b$ and $\rho(0, z) = \rho(X, z) = \rho_\pi(z)$, where ρ_b is the reservoir gas density and $\rho_\pi(z)$ is a one-dimensional density profile of the fluid near a hard wall.

B. DFT results

Within the present model the bulk critical temperature corresponds to $k_B T_c/\varepsilon = 1.414$. In our calculations we choose a relatively large value for the stripe potential, $\varepsilon_w \rho_w = \varepsilon \sigma^{-3}$, which at temperature $T = 0.95\,T_c$ ensures that the stripes are completely wet [9].

We next vary the distances between the stripes D_1 and D_2 and solve the Euler-Lagrange equation (21) at bulk saturation chemical potential $\beta\mu_{\mathrm{sat}} = -2.94$ corresponding to bulk coexistence with associated densities $\rho_l = 0.39\,\sigma^{-3}$ and $\rho_g = 0.13\,\sigma^{-3}$ of the liquid and gas bulk phases, respectively. Near a first-order bridging phase transition the density profile $\rho(\mathbf{r})$ obtained from Picard's iteration solution of the Euler-Lagrange depends on the initial configuration $\rho_i(\mathbf{r})$ of the fluid. If multiple solutions are present, that with the lowest
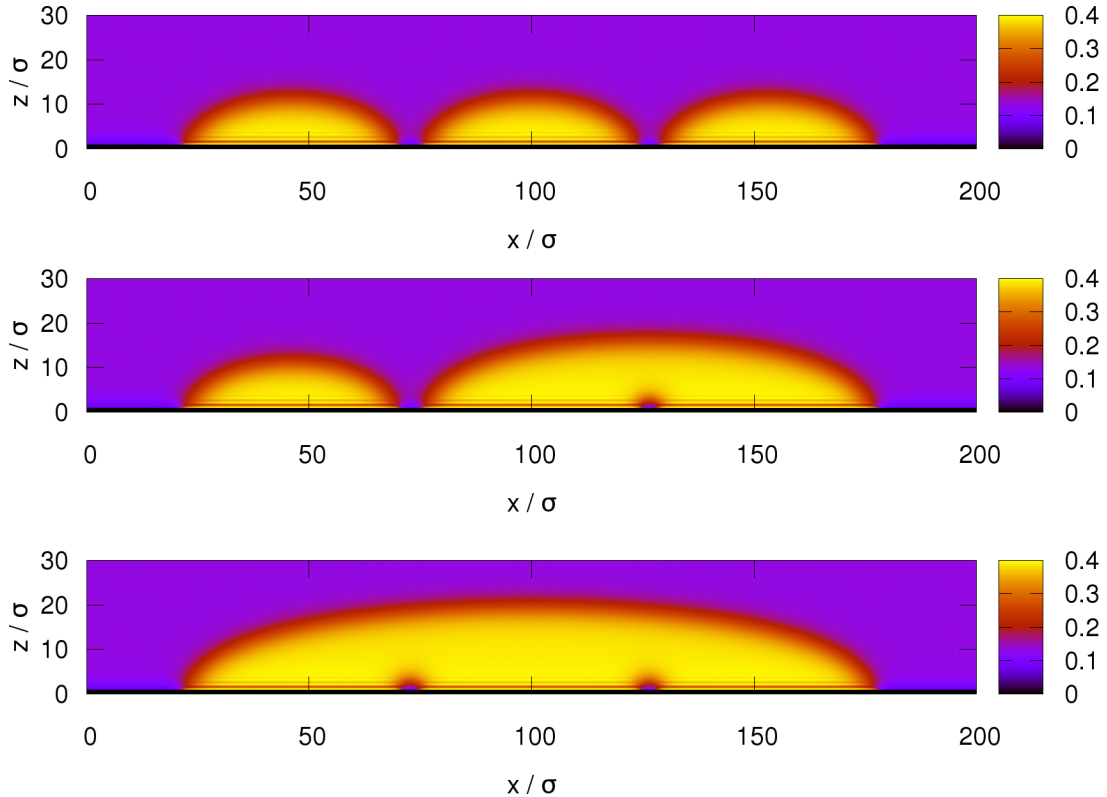

FIG. 4. DFT results for different equilibrium density profiles illustrating the microscopic structure underlying possible bridging morphologies of adsorbed liquid droplets. Here the width of the wetting stripes is $L = 50\,\sigma$, and the separations between them is (from top to bottom) (i) $D_1 = 4\,\sigma$ and $D_2 = 3.6\,\sigma$, (ii) $D_1 = 4\,\sigma$ and $D_2 = 3.4\,\sigma$, and (iii) $D_1 = 3.8\,\sigma$ and $D_2 = 3.6\,\sigma$.

grand potential corresponds to the equilibrium configuration. In order to converge to the isolated, double, and triple droplet configuration we chose (1) $\rho_i(\mathbf{r}) = \rho_b \exp[-\beta V(\mathbf{r})]$ where the system is filled by a gas, (2) the same plus a slab of liquid spanning two neighboring stripes, and (3) the same plus a slab of liquid spanning all three stripes. The height of the slabs was taken to be approximately a square root of their width.

We first discuss the "symmetric" model wall with equally separated stripes: $D_1 = D_2$. Figure 2 shows the dependence of the equilibrium grand potential as a function of $D = D_1 = D_2$. As can be seen, in this case the system undergoes a first-order phase transition at $D \approx 4\sigma$ from three droplets into one triple bridging droplet with two gaslike bubbles inside above the dry regions. Also shown is a curve corresponding to the grand potential of a metastable symmetry regime with two droplets. While this is never a global minimum of the grand potential the different branches of the free energy very nearly cross. This confirms the prediction that $D_B* > D_B$ and that the distance between their values is very small. In contrast, if we consider only a slightly "asymmetric" model with $D = D_1 = D_2 - \sigma$, a double bridging droplet configuration can

be stabilized within a narrow interval around $D = 4\sigma$ (see Fig. 3). The equilibrium density profiles illustrating all four possible droplet configurations are shown in Fig. 4.

Finally, in Fig. 5 we show the phase diagram in the D_1-D_2 plane. To determine this we performed an extensive number of DFT calculations by varying the values of D_1 and $D_2 \geqslant D_1$ within the interval $D_1 \in (1\sigma, 10\sigma)$. One can see that the phase diagram separates into four adsorption regimes with two triple points, which occur away from the diagonal. Note, however, that the distance between the locations of the triple points is less than one molecular diameter, consistent with the prediction that $D_B^* - D_B$ is molecularly small. As is evident, our microscopic DFT results confirm the predictions of the mesoscopic interfacial Hamiltonian model for the phase diagram structure. We are unable to verify the logarithmic dependence on the width L, which would require much larger systems; nevertheless, the value of $D_B \approx 4\sigma$ is completely consistent with the prediction (6) since $A/\gamma \approx \sigma^2$. We stress again, however, that it is the difference between D_B and D_B^* rather than their absolute values which determines the topology of the phase diagram.
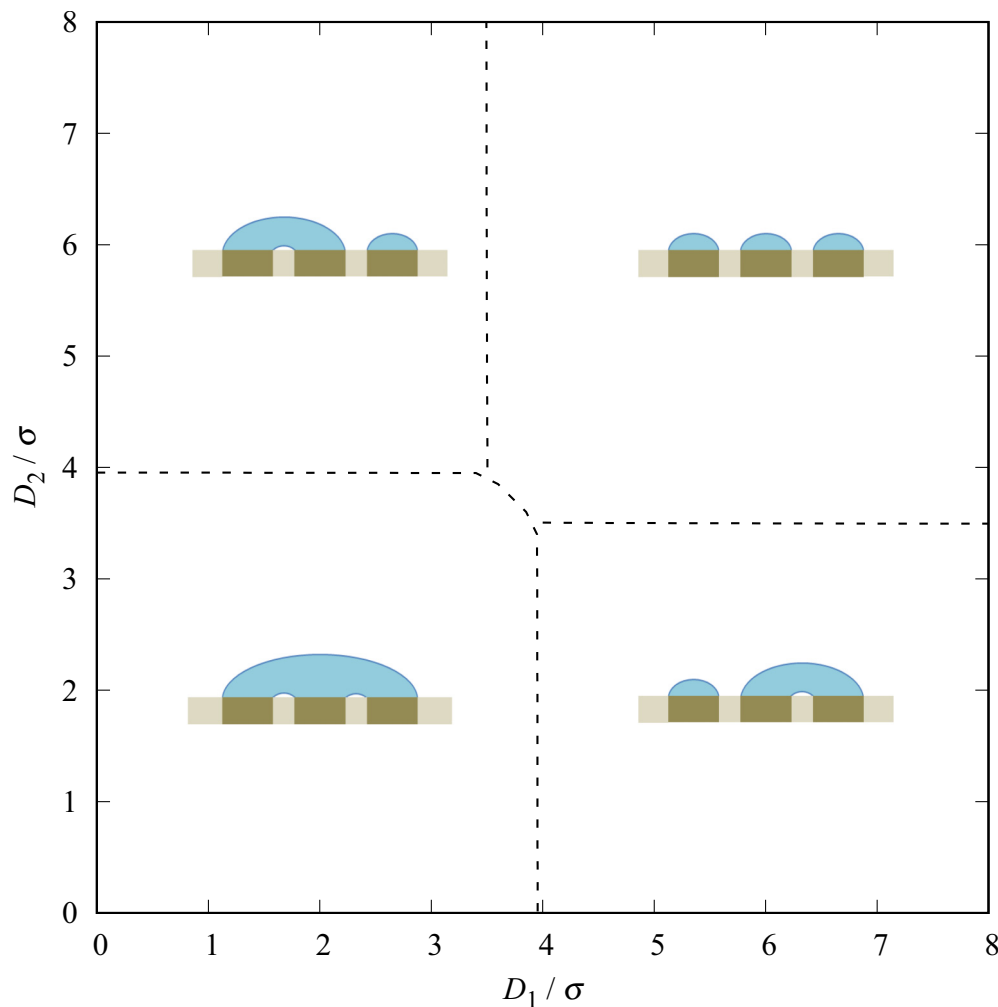

FIG. 5. Phase diagram in the D_1-D_2 plane showing the stable droplet configurations at bulk coexistence. Two triple points, occurring for $D_1 \neq D_2$, connect five separate first-order phase boundaries. The triple points lie very close to each other, reflecting the small difference between the equilibrium grand potential of the stable configuration and that of the metastable symmetry phase.

IV. CONCLUSION

In this paper we have used a microscopic DFT model to study bridging transitions on chemically patterned surfaces. We have focused on systems with long-ranged dispersion forces where there is a strong finite-size correction to the droplet free energy. The results confirm the predictions of simple interfacial Hamiltonian that bridging occurs only when the distance between the stripes is microscopically small. When the distance between the stripes D_1 and D_2 is varied the lines of phase coexistence intersect at two triple points. For the symmetric case $D_1 = D_2 \equiv D$ our results also confirm that the droplet configuration always has the symmetry of the substrate corresponding to either three isolated drops when D is large or a single triple drop when D is small. However, it is perhaps surprising that symmetry-broken configurations occur in a metastable part of the phase diagram which lies molecularly close to the equilibrium-bridging phase transition as predicted consistently both by the interfacial Hamiltonian model and DFT.

It is natural to speculate that very similar results occur when the number of stripes is increased. In particular, when the distance between the stripes is equal, the only possible configurations correspond to isolated drops (when D is large) or a single drop bridging across all the gaps (when D is microscopically small). As the number N of stripes increases, so does the height h_m of the single bridging droplet; at bulk coexistence we anticipate that $h_m \propto \sqrt{NL}$, since the size of the drop is approximately NL in width (the dependence on D may be dropped as $D \ll L$). It follows that in the thermodynamic limit corresponding to a periodic array of completely wet and partially wet or dry stripes, at bulk coexistence, there are only two equilibrium configurations: If D is large, there is a bound phase corresponding to isolated drops which sit above the wet regions. However, when D is microscopically small, these coalesce causing the liquid-gas interface to unbind from the surface. The simple interfacial Hamiltonian analysis of Sec. II predicts that this transition occurs when D takes a value $D_B = \sqrt{\frac{2A}{\gamma}} \frac{\ln L}{(1 - \cos\theta)}$ or equivalently when the fraction of the surface covered by the stripes is $f = 1 - O(\ln L/L)$. Since the liquid-gas interface unbinds from the substrate at this point it follows that we may interpret this as a first-order wetting transition induced by the chemical patterning of the substrate. The logarithmic dependence on L here, induced by the strong Casimir-like term in the drop free energy, corresponds to a correction of the prediction based on Cassie's law, which would require that the transition occurs when $D = 0$ or equivalently $f = 1$. Off coexistence this first-order wetting transition would also give rise to an associated prewetting line corresponding to thin-thick transitions in the adsorption of fluid when $D < D_B$. We intend to study this prediction for the periodic substrate using microscopic DFT in future work, as well as bridging transitions when drops are adsorbed on a surface decorated with circular patches requiring a 3D analysis.

[1] S. Y. Chou, P. R. Krauss, and P. J. Renstrom, Science **272**, 85 (1996).

[2] D. Quereé, Rep. Prog. Phys. **68**, 2495 (2005).

[3] D. Richard, C. Clanet, and D. Quereé, Nature (London) **417**, 6891 (2002).

[4] M. Napiorkowski, W. Koch, and S. Dietrich, Phys. Rev. A **45**, 5760 (1992).

[5] A. O. Parry, C. Rascón, and A. J. Wood, Phys. Rev. Lett. **85**, 345 (2000).

[6] D. B. Abraham and A. Maciołek, Phys. Rev. Lett. **89**, 286101 (2002).

[7] A. Milchev, M. Müller, K. Binder, and D. P. Landau, Phys. Rev. Lett **90**, 136101 (2003); Phys. Rev. E **68**, 031601 (2003).

[8] A. Malijevský and A. O. Parry, Phys. Rev. Lett. **110**, 166101 (2013).

[9] A. Malijevský and A. O. Parry, J. Phys: Condens. Matter **25**, 305005 (2013).

[10] A. O. Parry, A. Malijevský, and C. Rascón, Phys. Rev. Lett. **113**, 146101 (2014).

[11] G. Delfino and A. Squarcini, Phys. Rev. Lett. **113**, 066101 (2014).

[12] M. Tasinkevych and S. Dietrich, Eur. Phys. J. E **23**, 117 (2007).

[13] L. Bruschi, A. Carlin, and G. Mistura, Phys. Rev. Lett. **89**, 166101 (2002).

[14] A. O. Parry, C. Rascón, N. B. Wilding, and R. Evans, Phys. Rev. Lett. **98**, 226101 (2007).

[15] A. Malijevský and A. O. Parry, J. Phys: Condens. Matter **26**, 355003 (2014).

[16] M. C. Stewart and R. Evans, Phys. Rev. E **71**, 011602 (2005).

[17] A. Nold, A. Malijevský, and S. Kalliadasis, Phys. Rev. E **84**, 021603 (2011).

[18] S. L. Singh, L. Schimmele, and S. Dietrich, Phys. Rev. E **91**, 032405 (2015).

[19] A. Giacomello, L. Schimmele, and S. Dietrich, Proc. Natl. Acad. Sci. USA **113**, E262 (2016).

[20] S. Dietrich, in *Phase Transitions and Critical Phenomena*, edited by C. Domb and J. L. Lebowitz (Academic Press, New York, 1988), Vol. 12, p. 1.

[21] M. Schick, in *Liquids and Interfaces*, edited by J. Chorvolin, J. F. Joanny, and J. Zinn-Justin (Elsevier, New York, 1990), p. 419.

[22] G. Forgacs, R. Lipowsky, and T. M. Nieuwenhuizen, in *Phase Transitions and Critical Phenomena*, edited by C. Domb and J. L. Lebowitz (Academic Press, London, 1991), Vol. 14, p. 135.

[23] W. F. Saam, J. Low Temp. Phys. **157**, 77 (2009).

[24] P. Lenz and R. Lipowsky, Phys. Rev. Lett **80**, 1920 (1998).

[25] H. Gau, S. Herminghaus, P. Lenz, and R. Lipowsky, Science **283**, 486 (1999).

[26] A. Malijevský, A. O. Parry, and M. Pospíšil, Phys. Rev. E **96**, 032801 (2017).

[27] H. T. Dobbs and J. M. Yeomans, J. Phys.: Condens. Matter **4**, 10133 (1992).

[28] C. Bauer, T. Bieker, and S. Dietrich, Phys. Rev. E **62**, 5324 (2000).

[29] P. Hopkins, A. J. Archer, and R. Evans, J. Chem. Phys. **131**, 124704 (2009).

[30] A. Malijevský, Mol. Phys. **113**, 1170 (2015).

[31] A. Malijevský and A. O. Parry, Phys. Rev. E **92**, 022407 (2015).

[32] A. O. Parry, E. D. Macdonald, and C. Rascón, J. Phys: Condens. Matter **13**, 383 (2001).

[33] R. Lipowsky, Phys. Rev. Lett. **52**, 1429 (1984).

[34] V. Privman and M. E. Fisher, J. Stat. Phys. **33**, 385 (1983).

[35] R. Evans, Adv. Phys. **28**, 143 (1979).

[36] A. J. Archer, B. Chacko, and R. Evans, J. Chem. Phys. **147**, 034501 (2017).

[37] Y. Rosenfeld, Phys. Rev. Lett. **63**, 980 (1989).

[38] P. Tarazona, J. A. Cuesta, and Y. Martinez-Raton, in *Theory and Simulation of Hard-Sphere Fluids and Related Systems*, edited by A. Mulero, Lecture Notes in Physics Vol. 753 (Springer, Berlin, 2008), pp. 247–382.